Use of Capillary Electrophoresis for the Determination of the Conformation and Size of Individual Components in a Biopolymer Distribution: 1. Theory and Application to Amylose and Dextran

Andrew Ruddick[†] and David M. Goodall*

Department of Chemistry, University of York, York, YO10 5DD, U.K.

Received March 16, 1998; Revised Manuscript Received September 15, 1998

ABSTRACT: Derivatized low DP (degree of polymerization) oligomers of the polysaccharides amylose and dextran have been separated in aqueous solution at low pH using capillary electrophoresis and a novel model of polymer migration has been used to determine chain characteristics. The model is based on Debye−Hückel−Henry theory and a treatment of the polymers as simple freely rotating chains. Our results show that in the limit of zero ionic strength electrophoretic mobility is proportional to the inverse square root of the degree of polymerization, supporting the belief that amylose and dextran are random coils in aqueous solution. The characteristic ratio of amylose was found to be 3.2 using our model. Dextran chains were shown from electrophoretic mobilities to be more extended than amylose chains of equivalent degrees of polymerization, in agreement with results obtained from gel permeation chromatography.

Introduction

Polysaccharides are important components of biological systems. Amylose consists of linear 1,4-α-D-glucose chains (Figure 1) and is a component of starch, the major energy reserve of the higher plants. Enzymatically degraded starch (maltodextrin), which can contain varying quantities of amylose, is widely used as a gelling agent by the food industry, and its characterization is thus of commercial importance. The physical properties of amylose and its derivatives have been extensively studied in solution by viscometry, osmometry, and light scattering by a number of workers.[1−3] Dextran is produced by the action of dextran sucrases on sucrose and consists mostly of 1,6-linked α-D-glucose chains (Figure 1) with occasional branched units. Dextran is used in medicine as a blood plasma volume expander and to form iron−dextran for the treatment of anaemia; it also has applications in the cosmetics industry and as a calibration standard for gel permeation chromatography. Dextran has also been extensively studied in solution by light scattering and other methods.[4,5]

Capillary electrophoresis (CE) is a separation technique based on the differential migration of charged particles in an electric field.[6−8] A thin capillary (20−100-μm internal diameter) is filled with an electrolyte and a sample injected at one end. An electric field typically of 100−600 V cm^{-1} is applied across the capillary, and analyte species migrate according to their electrophoretic mobility μ, passing a detector (usually UV) at the end of the capillary. A bulk flow of the electrolyte toward the cathode also occurs, an effect known as electroosmotic flow. The apparent electrophoretic mobility μ_{app} of an analyte is thus the sum of its actual mobility and a term due to the bulk electrolyte flow.

Capillary electrophoresis is more than a high-resolution separation technique. It also provides a means to obtain physicochemical parameters such as ionic mobilities[9] and binding constants.[10] This paper describes the development of a simple analytical model relating electrophoretic mobility to the size and conformation of a polymer chain and its application to amylose and dextran.

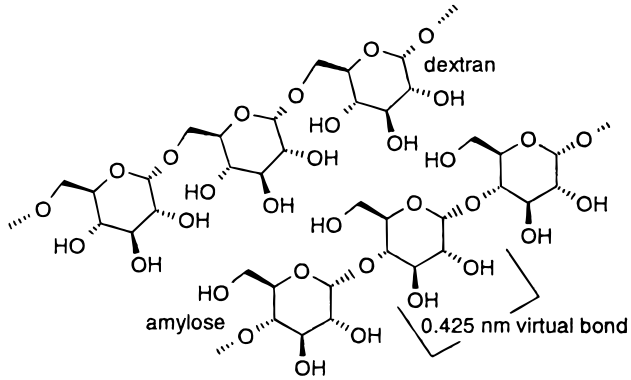

Figure 1. Structure of amylose and dextran.

Experimental Section

Materials. The amylose used in this study was Cerestar maltodextrin C*01906, which has a reported dextrose equivalent (DE) of 2−5%. This is a spray-dried maltodextrin obtained by degradation of gelatinized potato starch with α-amylase. It has a very broad molecular weight distribution and contains approximately 14% oligosaccharides with a DP < 10 but also high fractions with a MW up to 5×10^6 (DP 3×10^4; data from Cerestar). The high MW fraction is not seen under the conditions of our study. The dextran (purchased from Sigma Chemicals) was produced by *leuconostoc mesenteroides* strain B-512; it has an average MW of 19500 determined by low-angle laser light scattering (average DP = 120) and contains approximately 5% of non-1,6 linkages. Maltoheptose was supplied by Boehringer Mannheim GmbH; the dextran 10-mer was prepared using gel permeation chromatography by Dr. D. A. Ashford of the University of York Biology Department. 8-Aminonaphthalene-1,3,6-trisulfonic acid (ANTS) was obtained from Molecular Probes Inc.

Preparation of Electrolytes. Phosphate background electrolyte (BGE) solutions were prepared with phosphate concentrations of 20, 35, 50, 75, and 100 mM. All electrolytes

* To whom correspondence should be addressed.
[†] Present address: Department of Physics and Astronomy, University of Leeds, Leeds, LS2 9JT, U.K.

10.1021/ma980407c CCC: $15.00
Published on Web 11/06/1998

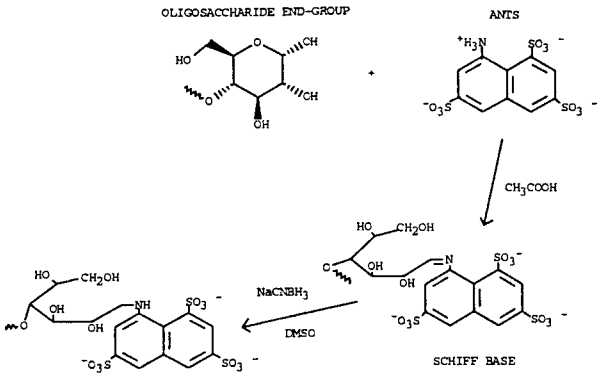

Figure 2. Derivatization of an oligosaccharide with ANTS.

contained a 10 mM concentration of protonated triethylamine (TEA), since the addition of TEA was found to improve reproducibility of the electroosmotic flow.[11] Solutions were titrated with 1 M NaOH solutions to pH 2.4. The ionic strengths, *I*, of the five BGE solutions were calculated using the IMPULSE program written by H. Poppe[12] and were found to be 13.5, 22.9, 33.9, 57.5, and 69.3 mmol kg^{-1} respectively.

Derivatization with ANTS. The procedure developed by Jackson[13] was used to tag the reducing ends of the sugar chains with ANTS; the reaction scheme is shown in Figure 2. The following procedure was followed for the derivatization of maltodextrin: (1) 20 mg of ANTS, 5 mg of maltodextrin, and 0.3 mg of maltoheptose were weighed into a 500-μL Eppendorf tube. (2) Then 200 μL of 17:3 v/v deionized water/acetic acid and 200 μL of 1 M sodium cyanoborohydride in dimethyl sulfoxide were added, and the mixture was heated in a water bath at 80 °C for 5.5 h, after which time all solid was dissolved. (3) An aliquot of this sample was diluted 10-fold with deionized water and used as the experimental sample. Both the concentrated and dilute solutions were stored in the freezer when not in use. The procedure for dextran derivatization was similar, using 20 mg of ANTS, 5 mg of dextran, and 0.4 mg of the dextran 10-mer standard. Heating was at 80 °C for 6.5 h, after which all solid was dissolved.

CE and GPC Experiments. All CE experiments were performed on a Beckman P/ACE CE system equipped with a diode array detector. The capillary was bare fused-silica, with a 75-μm internal diameter and 27-cm length; the distance to the detector was 20 cm. The capillary was thermostated at 25 °C; detection was at 220 nm, with a 2-Hz data collection rate. The sample of derivatized maltodextrin or dextran was injected hydrodynamically at 0.5 psi for 10 s; the run voltage was −5 kV. The data presented for maltodextrin and dextran were collected in one sequence; for a given BGE solution, three runs were performed with maltodextrin followed by three with dextran. The same run electrolyte vials were used for the six separations. The BGE solutions were used in the order 100, 50, 20, 75, and 35 mM phosphoric acid to eliminate any time-dependent effects. The capillary was rinsed with the appropriate electrolyte for 2 min between each injection. GPC experiments were performed on an Oxford GlycoSystems RAAM 2000 GlycoSequencer.

Results and Discussion

Theory. There is good evidence that amylose has a random coil conformation in solution, possibly with local helical structure.[14] Amylose can be considered in terms of the simple freely rotating chain model by describing the chain as a sequence of virtual bonds spanning from one glucosidic bridge to the next (Figure 1). This model was chosen because it allows the derivation of a simple analytical expression for mobility which accords with experimental observations. A critique of all aspects of our model will be given in the second paper of this series. The pyranose ring itself is assumed to be rigid, and chain flexibility is a result of rotation about the bridge oxygens. Throughout this paper we have taken the virtual bond length to be 0.440 nm.[15] Using the freely rotating chain model, it is possible to derive a relationship between the degree of polymerization (DP) and the electrophoretic mobility μ of the polymer, developing the model of Survay et al.[16] Henry[17] derived a general equation for the electrophoresis of a particle in an electrolyte:

$$\mu = \frac{2\epsilon\zeta f(\kappa a)}{3\eta} \tag{1}$$

where ϵ is the permittivity of the bulk electrolyte, ζ the zeta potential of the double layer around the migrating particle, η the electrolyte viscosity, and $f(\kappa a)$ a function of κ and a, the reciprocal of the double layer thickness and the hydrodynamic radius of the particle, respectively. In SI units κ is equivalent to the expression[18]

$$\kappa = \left[\frac{2000F^2I}{\epsilon RT}\right]^{1/2} \tag{2}$$

where F is the Faraday constant and I the electrolyte ionic strength. $f(\kappa a)$ is dependent on particle shape; for spherical particles it is given by[18]

$$f(\kappa a) = 1 + \frac{(\kappa a)^2}{16} - \frac{5(\kappa a)^3}{48} - \frac{(\kappa a)^4}{96} + \frac{(\kappa a)^5}{96} - \left[\frac{(\kappa a)^4}{8} - \frac{(\kappa a)^6}{96}\right]e^{\kappa a}\int_{\infty}^{\kappa a}\frac{e^{-t}}{t}\,dt \tag{3}$$

The zeta potential can be related to the particle charge Q by the expression[18,19]

$$\zeta = \frac{Q}{4\pi\epsilon a(1+\kappa a)} \tag{4}$$

Combining eqs 1 and 4 as described by Shaw,[19] Kálmán,[20] Gonnord,[21] and others gives eq 5 for the mobility of a migrating charged particle:

$$\mu = \frac{Qf(\kappa a)}{6\pi\eta a(1+\kappa a)} \tag{5}$$

The freely rotating chain model of a polymer in a random coil conformation[22] predicts that the mean square radius of gyration of a polymer chain, $\langle s^2\rangle_0$, is given by

$$\langle s^2\rangle_0 = \frac{1}{6}C_n n l_S^2 \tag{6}$$

where C_n is the characteristic ratio, n the number of virtual bonds in the chain, and l_S the length of a virtual bond. If we assume a linear relationship between the radius of gyration and hydrodynamic radius of a chain, $a = k\langle s^2\rangle_0^{1/2}$, we can write an equation relating the mobility of a chain to the chain length. For this work we have assumed $k = (5/3)^{1/2}$, which holds for the radius of gyration and radius of a solid sphere.[23] This leads to eq 7:

$$\mu = \frac{Qf(\kappa a)}{10^{1/2}\,\pi\eta C_n^{1/2} n^{1/2} l_S + {}^5/_3\,\pi\eta C_n n l_S^2 \kappa} \tag{7}$$

which, in the limit of zero ionic strength, and with chain

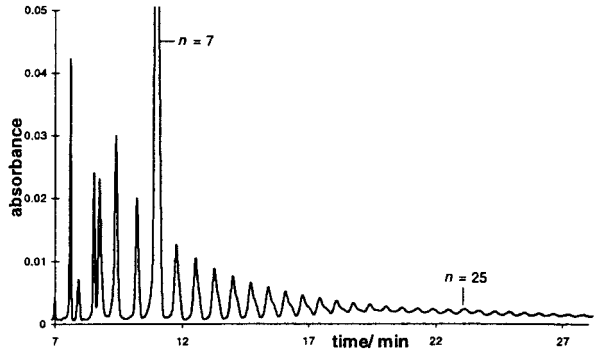

Figure 3. Electropherogram of ANTS−amylose in 100 mM phosphate BGE (pH 2.4): capillary length, 27 cm; length to detector, 20 cm; internal diameter, 75 μm; injection, 10 s at 0.5 psi; run voltage, −5 kV; detection, 220 nm.

length such that $C_n \rightarrow C_\infty$, reduces to

$$\mu_0 = \frac{Q}{10^{1/2}\,\pi\eta C_\infty^{1/2} n^{1/2} l_S} \tag{8}$$

Literature values for amylose C_∞ in water are ~5.[1,14,24]

Amylose Migration. Migration data for the ANTS-derivatized maltodextrin sample were collected in pH 2.4 phosphate BGE solutions of five different ionic strengths as described above. Figure 3 shows a typical electropherogram, with the spiked $n = 7$ peak clearly identifiable. Maximum visible DP of the linear chains varied between 35 and 43, depending on the phosphate concentration used. Data for $n \leq 10$ was discarded to ensure that any effect of the ANTS group on migration behavior would be negligible; the importance of this is discussed subsequently. The mean migration times for each set of triplicate injections were used to calculate apparent mobilities, μ_{app}, for each oligomer in a given electrolyte, using the equation

$$\mu_{app} = \frac{lL}{Vt} = \mu + \mu_{eo} \tag{9}$$

where l is the length to the detector, L the capillary length, V the applied voltage, t the migration time, and μ_{eo} the electroosmotic flow mobility. Since the experiments were run with the anode at the detector end of the capillary, it was not possible to use a neutral marker to determine the magnitude of the electroosmotic flow (EOF) in the same run. Instead, its value was taken to be the y-intercept of μ_{app} against $1/n^{1/2}$ graphs. These extrapolated values for μ_{eo} were in the range $2.0-2.7 \times 10^{-9}$ m^2 V^{-1} s^{-1}. A mesityl oxide marker was used to measure the magnitude of μ_{eo} directly in the 20 mM phosphate with the detector at the cathode; the mean value was 2.0×10^{-9} m^2 V^{-1} s^{-1} (RSD 25%, seven measurements). The fact that extrapolated and directly observed values of μ_{eo} are seen to be in good agreement here validates the more general use of the extrapolation method. The electrophoretic mobility is predicted to be proportional to $1/n^{1/2}$ at zero ionic strength (eq 8). In practice, this relationship gave good straight line fits to the data at all ionic strengths (Figure 4). This is somewhat surprising in view of eq 7; for 20 mM phosphate, substituting values into this equation gives

$$\mu = \frac{zef(\kappa a)}{(8.70 \times 10^{-12})n^{1/2} + (1.72 \times 10^{-12})n} \tag{10}$$

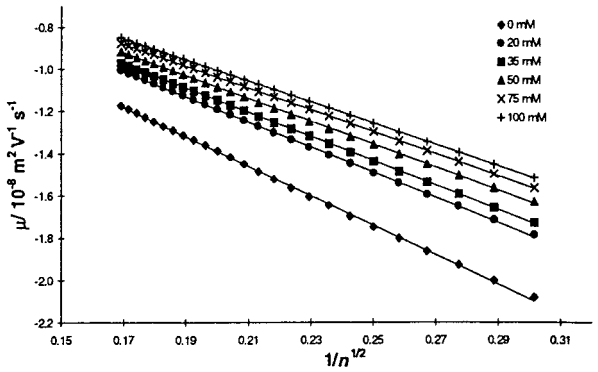

Figure 4. Electrophoretic mobilities as a function of $1/n^{1/2}$ for ANTS−amylose oligomers.

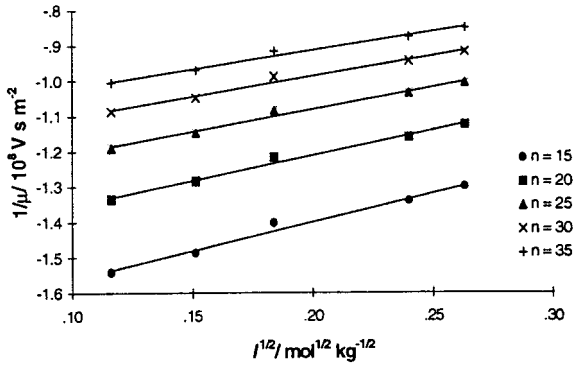

Figure 5. Plot of $1/\mu$ against $I^{1/2}$ for selected ANTS−amylose oligomers, DP = 11−35.

with the values of the variables taken to be $\eta = 8.91 \times 10^{-4}$ kg m^{-1} s^{-1}, $C_\infty = 5$, $l_S = 0.440$ nm, and $\kappa = 0.382$ nm^{-1} (eq 2). This suggests that μ should not scale linearly with $1/n^{1/2}$ in any of the electrolytes in our study. The disparity between theory and experimental observation is discussed subsequently, when the extrapolation of our data to zero ionic strength has been considered.

If the value of $f(\kappa a)$ is considered to be constant, the inverse of electrophoretic mobility is predicted to be a linear function of the square root of the BGE ionic strength; combination of eqs 2 and 5 gives

$$\frac{1}{\mu} = \frac{6\pi\eta a^2 (2000F^2/\epsilon RT)^{1/2} I^{1/2}}{zef(\kappa a)} + \frac{6\pi\eta a}{zef(\kappa a)} \tag{11}$$

From eqs 2 and 3 it can be deduced that the variation in $f(\kappa a)$ is indeed small over the range of concentrations and hydrodynamic radii concerned. κ was calculated using eq 2; a was estimated from eq 6, assuming a value of C_∞ of 5 and a value of l_S of 0.440 nm. The greatest variation in the value of κa for migration of a given oligomer is 0.914 (20 mM phosphate) to 2.07 (100 mM) for the $n = 35$ chain. This gives a change in the value of $f(\kappa a)$ from 1.02 to 1.07;[18] its approximation to a constant appears reasonable. This being the case, a set of mobilities corrected to zero ionic strength, μ_0, can be obtained by plotting the inverse of the electrophoretic mobilities shown in Figure 4 against $I^{1/2}$ and extrapolating to $I^{1/2} = 0$, as illustrated in Figure 5. The results of this procedure are given in Table 1. An experimental value of C_∞ can then be extracted by plotting these data against $1/n^{1/2}$ as shown in Figure 4 and using eq 8 to determine C_∞ from the slope of the graph.

To calculate C_∞, we assume the values $l_S = 0.440$ nm, $\eta = 8.91 \times 10^{-4}$ kg m^{-1} s^{-1}, $e = 1.602 \times 10^{-19}$ C, and z

Table 1. Results of Regression Analysis To Determine μ_0 for ANTS−amylose and ANTS−dextran Oligomers

n	amylose $\mu_0 \pm t_{95}s_{\mu 0}/10^{-8}$ m^2 V^{-1} s^{-1}	dextran $\mu_0 \pm t_{95}s_{\mu 0}/10^{-8}$ m^2 V^{-1} s^{-1}
11	−2.079 ± 0.126	
12	−2.000 ± 0.120	−1.882 ± 0.158
13	−1.927 ± 0.109	−1.809 ± 0.151
14	−1.862 ± 0.108	−1.747 ± 0.140
15	−1.802 ± 0.105	−1.689 ± 0.132
16	−1.748 ± 0.097	−1.638 ± 0.121
17	−1.698 ± 0.082	−1.589 ± 0.113
18	−1.647 ± 0.077	−1.545 ± 0.105
19	−1.605 ± 0.074	−1.504 ± 0.098
20	−1.563 ± 0.076	−1.465 ± 0.094
21	−1.522 ± 0.075	−1.429 ± 0.089
22	−1.486 ± 0.051	−1.396 ± 0.085
23	−1.451 ± 0.074	−1.364 ± 0.082
24	−1.418 ± 0.073	−1.337 ± 0.079
25	−1.389 ± 0.071	−1.309 ± 0.076
26	−1.361 ± 0.071	−1.286 ± 0.075
27	−1.337 ± 0.068	−1.262 ± 0.076
28	−1.316 ± 0.071	−1.240 ± 0.076
29	−1.290 ± 0.070	−1.218 ± 0.075
30	−1.271 ± 0.070	−1.198 ± 0.076
31	−1.250 ± 0.068	−1.179 ± 0.077
32	−1.229 ± 0.066	−1.160 ± 0.077
33	−1.208 ± 0.065	−1.142 ± 0.078
34	−1.190 ± 0.066	−1.124 ± 0.081
35	−1.174 ± 0.066	−1.109 ± 0.083
36		−1.095 ± 0.086
37		−1.080 ±0.079
38		−1.066 ± 0.089
39		−1.052 ± 0.091
40		−1.035 ± 0.108
41		−1.012 ± 0.110

$= -3$, with the ANTS group fully ionized. This being the case, following linear regression of the data given in Table 1, eq 8 gives a value of $C_\infty = 3.16 \pm 0.02$. The quoted error limits indicate the 95% confidence intervals of the above linear regression and do not include any estimates of systematic error or account for the error already associated with the μ_0 values, as discussed below. In a review of computer models of amylose,[25] the Arnott−Scott virtual bond length of 0.440 nm is seen to be approximately at the center of a distribution of values found in the literature. Systematic errors in C_∞ of ∼±10% are therefore possible from 5% changes in l_S between the center and extremes of the distribution. Literature values for C_∞ of the unperturbed amylose chain are in the range ∼5−6.[1,14,24] These values were determined from light-scattering and viscosity measurements made in 0.33 M KCl, said to be a θ solvent for amylose. Our value of $C_\infty = 3.2$ appears to show a significant difference from the literature values. As stated previously, the confidence intervals on this value will be much wider than the limits given above, since each μ_0 value itself contains a degree of uncertainty (Table 1). In the worst case, with μ_0 values at the extremes of their 95% confidence limits, this would lead to confidence intervals for C_∞ of approximately ±50%, although this is highly unlikely to be the case given the low scatter evident in Figure 4. It appears reasonable to say that although the discrepancy between calculated and experimental C_∞ values may be partially attributable to experimental error, a real difference exists. This is discussed subsequently. Measurements made in pure water give a value of C_∞ of ∼11.7.[2] Since the experiments in this study were carried out in pH 2.4 phosphate−TEA, it is unlikely that we can regard the value of C_∞ obtained either as a truly unperturbed value or as a value in pure water; however, the excluded volume effect will be small in the low DP chains involved in this study. For example, Brant and Min[3] calculate an expansion coefficient in water of $\alpha^2 = 1.26$ for sodium carboxymethylamylose with an average molecular weight of $5.8 \times 10^4 \pm 3\%$ (DP 360), and the chains in our study are an order of magnitude shorter. Nakata et al.[26] suggest that the excluded volume effect in DMSO is small up to DP = 40 based on a model of amylose as a helical wormlike molecule. In addition, the observed $\langle s^2 \rangle_0^{1/2} \propto n^{0.5}$ relationship is itself evidence for the θ state; when the excluded volume effect is large, the power of n to which $\langle s^2 \rangle_0^{1/2}$ is proportional increases to a value greater than 0.5.[27] We can therefore be confident that our result closely approximates an unperturbed value for aqueous solvents.

The excellent straight line relationship between μ_0 against $1/n^{1/2}$ is surprising in the case of the low DP chains in this experiment; the freely rotating chain model predicts that C_n in the range $n = 11-35$ should not have reached its limiting value for a value of C_∞ between 3 and 5. Urbani and Cesáro[28] performed conformational energy calculations on amylose which suggest that in water C_n for amylose does not exceed 95% of C_∞ until $n > 300$. This is in agreement with calculations by Brant and Dimpfl,[29] using a model of the random coil which accounts for bond rotational interdependence at the glycosidic bridges. However, so far as we are aware all viscometric and light-scattering measurements on amylose to date have been carried out with high MW samples; the behavior of amylose oligomers of very low MW has not been experimentally verified.

Even when the variation of C_n with n was neglected, it was noted earlier that eq 7 implies that graphs of μ against $1/n^{1/2}$ at a given ionic strength should not be linear for $I > 0$ because of the term in n in the denominator. Thus, the effect of the electrolyte ionic strength is smaller than that predicted by theory. One inherent limitation in our theory is the use of the Debye−Hückel approximation in the derivation of eqs 1 and 4.[18] This limits the applicability of the equation to zeta potentials of less than 25.7 mV/z, where z is the charge on the ion in units of e. On the basis of our calculations of hydrodynamic radii, zeta potentials somewhat greater than this exist for many of the polysaccharide chains in our study. Numerical methods have been employed for the accurate determination of zeta potentials greater than the 25.7 mV/z limit,[30] and these may be usefully applied to our samples in future work. In light of this discussion it may be appropriate to regard our $1/\mu$ against the $I^{1/2}$ ionic strength correction as an empirical correction which has some support from theory, rather than a process which has unequivocal theoretical justification.

Other attempts to model amylose mobilities are scarce. Chiesa and Horvàth[11] discuss an empirical relationship between $1/\mu$ and n; data for oligomers between $n = 2$ and $n = 24$ are included in their analysis. However, inspection of their data (Figure 8 on p 346 of the reference) shows that the data points increasingly fall below the line of best fit as n increases; no physical basis is proposed for this relationship. The relationship $\mu = CqM^{-2/3}$, where C is a constant, q is the charge, and M is the molecular mass, is also discussed by Chiesa and Horvàth. This equation was described by Offord[31] to account for peptide mobilities in paper electrophoresis. Chiesa and Horvàth show plots of their amylose

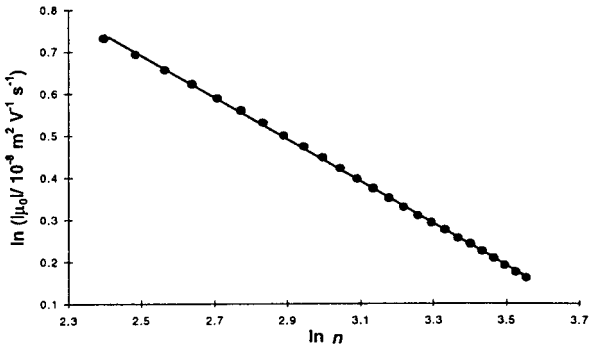

Figure 6. ln $|\mu_0|$ against ln n for ANTS−amylose oligomers, DP > 10.

mobilities versus $M^{-2/3}$. Again, the data appear to deviate from the fit line in a systematic manner, although this may be within experimental error.

Oefner and Chiesa[32] state that the slope of a log−log plot of electrophoretic mobility versus molecular weight is "almost exactly" −2/3 for malto-oligosaccharides with n between 2 and 37. Regression analysis of ln $|\mu_0|$ against ln n for our data with DP > 10 (Figure 6) gives a slope of -0.501 ± 0.004 with $R^2 = 1.000$. For $n > 2$ regression of ln $|\mu|$ versus ln n for the 100 mM data gives a slope of -0.56 ± 0.02 with $R^2 = 0.991$. Inspection of a plot of these data shows that it is not a straight line (i.e., the proportionality between μ and n changes as n increases). It should be noted that there is also a smaller but consistent deviation from a straight line when the data are restricted to $n > 10$. Only in the limit of zero ionic strength is this deviation absent (Figure 6), although this may in part be attributable to the greater uncertainty in the extrapolated mobilities masking any deviation from linearity. Figure 6 does, however, show excellent agreement with the $n^{-0.5}$ dependency of μ_0 predicted by the freely rotating chain model.

The disparity between the results presented here and those of Chiesa may therefore be a consequence of the inclusion of data for very low DP chains in Chiesa's analysis; the effect of the ANTS end group and the rapid change in the value of C_n over this DP range results in deviation from the simple limiting C_n theory. However, it should be noted that the apparent linear relationship between μ and $M^{-2/3}$ seen by Chiesa is not at all evident in our data. Additionally, the effect of the ionic strength is neglected by Chiesa. Equation 7 predicts that mobility should vary as $1/(an^{1/2} + bn)$, where a is a constant and b is an ionic-strength-dependent parameter. It is clear that any unambiguous comparison between different mobility models must be made in the limit of zero ionic strength, as previously discussed for peptide mobility modeling.[16]

Dextran Migration. Mobility data for the ANTS-derivatized dextran sample were collected in a manner identical to the maltodextrin, as outlined in the Experimental Section. It is not possible to treat dextran as a series of identical virtual bonds in the same manner as amylose; however, it is still reasonable to suppose that $\langle s^2 \rangle_0$ will scale with n and as a result that $\mu_0 \propto 1/n^{1/2}$, since this is a general result for a linear flexible chain.[33] A value of $l_S C_\infty^{1/2}$ can thus be calculated in an analogous fashion to the calculation of C_∞ for amylose, and the migration of the two systems can be compared.

Figure 7 shows an electropherogram of the derivatized dextran migrating in the 100 mM, pH 2.4 phosphate BGE. The mean magnitude of the electroosmotic flow in each electrolyte was determined as described previously, and the corrected mobilities are plotted in Figure 8. The EOF-corrected data for all five electrolytes are extrapolated to zero ionic strength; the resulting values of μ_0 are given in Table 1 and plotted in Figure 8.

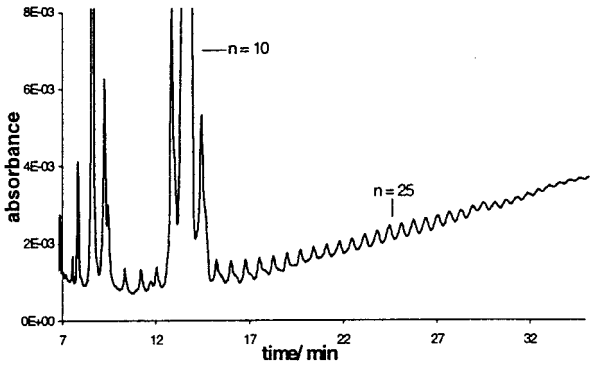

Figure 7. Electropherogram of ANTS−dextran in 100 mM phosphate 10 mM triethylamine (pH 2.4) BGE: capillary length, 27 cm; length to detector, 20 cm; diameter, 75 μm; injection, 10 s at 0.5 psi; run voltage, −5 kV; detection, 220 nm.

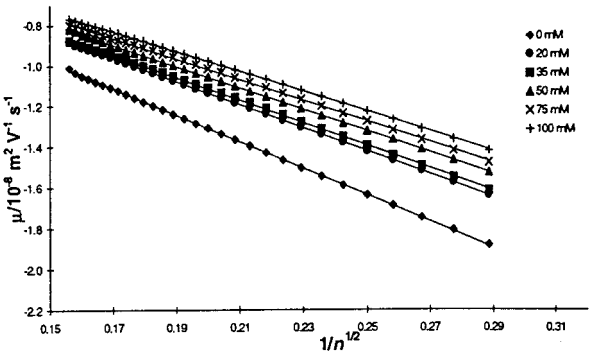

Figure 8. Electrophoretic mobilities as a function of $1/n^{1/2}$ for ANTS−dextran oligomers.

A plot of ln $|\mu_0|$ versus ln n for DP > 10 has a slope of -0.497 ± 0.003, implying that $\langle s^2 \rangle_0^{1/2} \propto n^{0.50} \propto M_w^{0.50}$, and hence that the linear random coil is a good model for the dextran with a DP = 12−41 in our sample. From light-scattering data, Nordmeier found the relationship $\langle s^2 \rangle_0^{1/2} = 6.33 \times 10^{-2} M_w^{0.427}$ in the MW range (8×10^4)−(1×10^8) [DP = 500−(6×10^5)]. The exponent of 0.427 suggests a branched structure. These data are consistent with the electropherogram of Figure 7, which shows noticeable shoulders to the main peaks. These are probably attributable to branched molecules, which have no effect on our analysis since we include only the peaks attributable to linear molecules. The light-scattering method does not allow discrimination of individual chains and gives an average result over all chains.

The gradient of the graph of μ_0 against $1/n^{1/2}$ yields a value of $l_S C_\infty^{1/2}$ of $(8.35 \pm 0.04) \times 10^{-10}$ m, based on eq 8; this compares with the value of $(7.82 \pm 0.08) \times 10^{-10}$ m obtained for amylose, implying that the 1,6-linked dextran chain is more extended than the 1,4-linked amylose chain. This is in agreement with Rees and Scott[34] who carried out computer-modeling calculations on 1,2-, 1,3-, 1,4-, and 1,6-linked polyglucan chains. Their results suggest that the dextran chain is more flexible but on average more extended than the amylose chain, in accordance with our experimental data.

The migration behavior of amylose and dextran in CE is also in accordance with their separation by gel

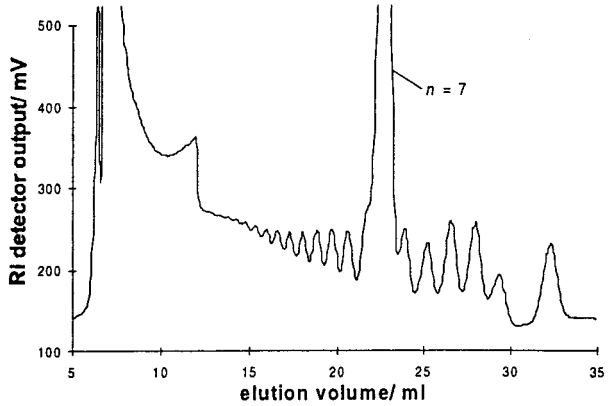

Figure 9. GPC trace of 2.0 mg mL^{-1} of amylose, flow rate of 160 μL min^{-1}, RI detection (courtesy of Dr. D. A. Ashford).

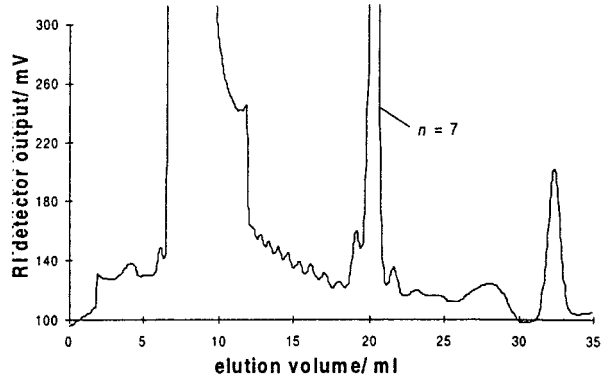

Figure 10. GPC trace of 2.1 mg mL^{-1} of dextran, flow rate of 160 μL min^{-1}, RI detection (courtesy of Dr. D. A. Ashford).

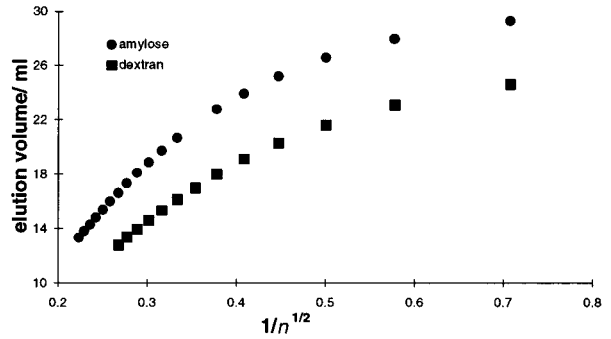

Figure 11. Elution volume as a function of $1/n^{1/2}$ for amylose and dextran oligomers separated by GPC.

permeation chromatography (GPC). In a GPC experiment a dextran chain would be expected to elute before an amylose chain of equal DP, and this is indeed the case. Figures 9 and 10 show GPC traces of our amylose and dextran samples spiked with heptamer. A given dextran chain appears to have a radius equivalent to an amylose chain with a DP 1.3 times greater e.g., a DP = 15 amylose chain has a dextran calibration of DP = 11.3. Inspection of Table 1 suggests a scaling factor of approximately 1.1 for the amylose and dextran μ_0 data. A graph of the eluted solvent volume, inversely proportional to analyte radius, against $1/n^{1/2}$ is shown in Figure 11. Although only low DP chains could be visualized by GPC, the graph does appear to show a linear relationship between the inverse of the particle radius and $1/n^{1/2}$ developing as DP increases, in accordance with the results of our CE experiments.

Acknowledgment. We acknowledge the assistance of Dr. D. A. Ashford, Department of Biology, University of York, for performing the GPC experiments. Additionally, we thank EPSRC and Zeneca LifeScience Molecules for their financial support.

References and Notes

(1) Goebel, K. D.; Brant, D. A. *Macromolecules* **1970**, *3*, 634.
(2) Ring, S. G.; l'Anson, K. J.; Morris, V. J. *Macromolecules* **1985**, *18*, 182.
(3) Brant, D. A.; Min, B. K. *Macromolecules* **1969**, *2*, 1.
(4) Nordmeier, E.; Xing, H.; Lechner, M. *Makromol. Chem.* **1993**, *194*, 2923.
(5) Nordmeier, E. *J. Phys. Chem.* **1993**, *97*, 5770.
(6) Grossman, P. D.; Colburn, J. C. *Capillary Electrophoresis, Theory and Practice*; Academic Press: San Diego, CA, 1992.
(7) Weinberger, R. W. *Practical Capillary Electrophoresis*; Academic Press: Boston, 1993.
(8) Landers, J. P., Ed. *Handbook of Capillary Electrophoresis*; CRC Press: Boca Raton, FL, 1992.
(9) Survay, M. A.; Goodall, D. M.; Wren, S. A. C.; Rowe, R. C. *J. Chromatogr.* **1993**, *636*, 81.
(10) Penn, S. G.; Bergström, E. T.; Knights, I.; Liu, G.; Ruddick, A.; Goodall, D. M. *J. Phys. Chem.* **1995**, *99*, 3875.
(11) Chiesa, C.; Horváth, C. *J. Chromatogr.* **1993**, *645*, 337.
(12) Poppe, H. *Anal. Chem.* **1992**, *64*, 1908.
(13) Jackson, P. *Biochem. J.* **1990**, *270*, 705.
(14) Banks, W.; Greenwood, C. T. *Starch and its Components*; Edinburgh University Press: Edinburgh, 1975; Chapter 4.
(15) Arnott, S.; Scott, W. E. *J. Chem. Soc., Perkin Trans. 2* **1972**, 324.
(16) Survay, M. A.; Goodall, D. M.; Wren, S. A. C.; Rowe, R. C. *J. Chromatogr.* **1996**, *741*, 99.
(17) Henry, D. C. *Proc. R. Soc. (London) Ser. A* **1931**, *133*, 106.
(18) Hunter, R. J. *Zeta Potential in Colloid Science—Principles and Applications*, Academic Press: New York, 1981.
(19) Shaw, D. J. *Electrophoresis*; Academic Press: London, New York, 1969; p 17.
(20) Kálmán, F.; Ma, S.; Fox, R. O.; Horváth, C. *J. Chromatogr.* **1995**, *705*, 135.
(21) Gonnord, M. F.; Collet, J. *J. Chromatogr.* **1993**, *645*, 327.
(22) Flory, P. J. *Statistical Mechanics of Chain Molecules*; Hanser Publications: New York, 1988.
(23) Atkins, P. W. *Physical Chemistry*, 4th ed.; Oxford University Press: Oxford, 1990; p 698.
(24) Jordan, R. C.; Brant, D. A. *Macromolecules* **1980**, *13*, 491.
(25) French, A. D.; Murphy, V. G. *Carbohydr. Res.* **1973**, *27*, 391.
(26) Nakata, Y.; Kitamura, S.; Takao, K.; Norisuye, T. *Polym. J.* **1994**, *26*, 1085.
(27) Utiyama, H.; Utsumi, S.; Tsunashima, Y.; Kurata, M. *Macromolecules* **1978**, *11*, 506.
(28) Urbani, R.; Cesàro, A. *Polymer* **1991**, *32*, 3013.
(29) Brant, D. A.; Dimpfl, W. L. *Macromolecules* **1970**, *3*, 655.
(30) O'Brien, R. W.; White, L. R. *J. Chem. Soc., Faraday Trans. 2* **1978**, *74*, 1607.
(31) Offord, R. E. *Nature* **1966**, *211*, 591.
(32) Oefner, P. J.; Chiesa, C. *Glycobiology* **1994**, *4*, 397.
(33) Tanford, C. *Physical Chemistry of Macromolecules*; John Wiley and Sons: New York, 1965.
(34) Rees, D. A.; Scott, W. E. *J. Chem. Soc. B* **1971**, 469.

MA980407C